ENVIRONMENTAL ENGINEERING SCIENCE
Volume 30, Number 9, 2013

DOI: 10.1089/ees.2012.0056

Removal of Carbamazepine from Water by a Novel TiO_2–Coconut Shell Powder/UV Process: Composite Preparation and Photocatalytic Activity

Majeda Khraisheh,[1,*] Jongkyu Kim,[2] Luiza Campos,[2] Ala'a H. Al-Muhtaseb,[3] Gavin M. Walker,[4,5] and Mohammad AlGhouti[6]

Departments of [1]Chemical Engineering and [6]Biology & Environmental Science, Qatar University, Doha, Qatar.
[2]Department of Civil, Environmental, and Geomatic Engineering, University College London, London, United Kingdom.
[3]Department of Petroleum and Chemical Engineering, Faculty of Engineering, Sultan Qaboos University, Muscat, Oman.
[4]School of Chemistry and Chemical Engineering, Queen's University Belfast, Belfast, United Kingdom.
[5]Department of Chemical and Environmental Sciences, Materials Surface Science Institute, University of Limerick, Limerick, Ireland.

Received: February 14, 2012 *Accepted in revised form: April 15, 2013*

Abstract

A novel TiO_2–coconut shell powder (TCNSP) composite, prepared by the controlled sol-gel method with a subsequent heat treatment, was investigated as an innovative photocatalytic absorbent for the removal of carbamazepine (CBZ). CBZ is used worldwide as an antiepileptic drug, which has recently been recognized as an important organic pollutant increasingly found in wastewaters from urban areas and other aquatic environments. The granulation process was performed by using a semiautomated mass production line to produce sufficient quantities of TCNSP composites, possessing sufficient crush strength for commercialization. Physical properties of the TCNSP composite such as crystallinity, morphology, crush strength, and the Brunauer-Emmett-Teller (BET)–specific surface area were controlled by the mass ratio of titanium dioxide sol and coconut shell powder (CNSP). Calcination at 700°C produced anatase phase TiO_2 in the TCNSP composites with a BET high surface area of 454 m^2/g. Anatase crystallite size of the TCNSP composite increased from 2.37 to 15.11 nm with increasing calcination temperature from 500°C to 800°C. Calcinated TCNSP composites had higher CBZ removal efficiency (98%) than pure TiO_2 (23%) and CNSP (34%) within a 40-min reaction time. Optimization of this innovative adsorption/photocatalytic process was obtained by a response surface methodology and a central composite design model, which indicated that this novel and sustainable technology was successful in removing CBZ from a solution.

Key words: drug; granulation; photocatalytic degradation; semiautomated mass production line; TiO_2–coconut shell powder composite

Introduction

In recent years, heterogeneous photocatalysis in the presence of TiO_2 has attracted a great deal of attention for the purification of water (Valencia *et al.*, 2011). TiO_2 photocatalysis accelerates the photochemical transformation by the action of a catalyst, which is active, low in cost, nontoxic, and chemically stable over a wide pH range (Nieto-Suárez *et al.*, 2009). However, the use of TiO_2 photocatalysis for commercial or industrial applications is limited for a number of reasons. Primarily, TiO_2 is only efficient for low concentrations (ppm to ppb levels) of contaminants in water. The adsorption efficiency of TiO_2 can also be low due to its relatively small specific surface area (Raj and Vismanathan, 2009). Furthermore, TiO_2 powder nanoparticles can easily agglomerate, which reduces the photonic efficiency for most degradation processes and requires costly microfiltration processes for recovering micron-sized aggregated particles from water decontaminated by TiO_2 slurry (Liu *et al.*, 2009).

To increase the surface area of the catalyst and decrease the limitations imposed by filtration of a fine powder, TiO_2 has been supported on a range of different materials such as zeolite, alumina, and stainless steel (Chen and Dionysiou, 2006; Shankar *et al.*, 2006; Bouna *et al.*, 2011; Yu *et al.*, 2012). Among these materials, activated carbon is widely used as a support for both gas- and liquid-phase reactions due to the high surface area (Walker and Weatherley, 1997; Li *et al.*, 2008; Iwasaki *et al.*, 2010; Le *et al.*, 2012), and chemical inertness at low

**Corresponding author:* Department of Chemical Engineering, Qatar University, P.O. Box 2713, Doha, Qatar. *Phone:* +974-33166752; *Fax:* +974-44034001; *E-mail:* m.khraisheh@qu.edu.qa

temperatures (Iwasaki *et al.*, 2010). Another advantage of supporting TiO_2 on activated carbon is that a reduction of intermediates during photocatalysis is often observed (Yoneyama and Torimoto, 2010). However, most of the TiO_2/activated carbon mixtures are prepared by multistage processes, whereby the commercially made activated carbon is formed from a carbonaceous precursor followed by the deposition or synthesizing of TiO_2, which is time and energy intensive (Tamai *et al.*, 2002; Li *et al.*, 2007).

The coconut shell is a particularly interesting raw material as a precursor of carbon due to the excellent natural structure and low ash content (Su *et al.*, 2003). In addition, it is a waste product from agriculture and food processing operations with little or no economic value and its disposal is not only costly, but may also cause environmental concern (Li *et al.*, 2008; Acharya *et al.*, 2009). Conversion of such a waste material into usable material for water purification for the treatment of industrial and municipal effluents would add value to these agricultural commodities.

Carbamazepine (CBZ; $C_{15}H_{12}N_2O$), is an antiepileptic drug currently prescribed for treatment of seizure disorders, chronic pain, and for psychopharmacotherapy (Vogna *et al.*, 2004) which is commonly found in environmental matrices. It passes through wastewater treatment plants (WWTPs) almost completely unaffected and has been found to be highly persistent in the environment (Calisto and Esteves, 2012). The sludge produced in WWTPs is commonly applied in agricultural fields as a soil amendment; the occurrence of pharmaceuticals, in soils, with low sorption affinity can contribute to the contamination of the adjacent surface and ground waters through run-off and infiltration.

The global production of CBZ is estimated to be 1014 t/year (Zhang *et al.*, 2008). CBZ has been found in WWTP effluents around the world typically at a concentration of hundreds of nanograms per liter; however, the concentration can sometimes be in the micrograms per liter range. The aim of this present work is to prepare novel TiO_2 with coconut shell powder (TCNSP) composites by using a semiauto mass production line (AMPL) as a granulation process. The effect of processing parameters (i.e., calcination temperature and coconut shell powder [CNSP] loading amount) was examined. The use of TCNSP composites in the photocatalytic degradation of CBZ was also assessed. The effect of the processing parameters was evaluated by using a response surface methodology (RSM) and a central composite design model (CCD).

Materials and Methods

Synthesis of TCNSP composite

All the chemicals used in this work were of analytical grade. The water used in the preparation of all the solutions was obtained from an Ondeo water purification system. CNSP was used as the main raw material in the production of TCNSP (Table 1). A novel TCNSP composite was synthesized by coating raw CNSP (particle size of 0.2–0.4 mm) with TiO_2 via the acid-catalyzed sol-gel method (Li *et al.*, 2007). The TCNSP composites were prepared using the following procedure: 34.04 mL Titanium-n-butoxide $Ti(Obu)_4$ and 10.4 mL diethanolamine $NH(C_2H_4OH)_2$ were dissolved together in 259.28 mL ethanol, and the solution was stirred continuously for 1 h at room temperature. This was followed by the addition of different amounts of CNSP. In this step, the raw CNSP was previously washed with deionized water and dried at 110°C for 48 h and crushed with a roller mill (RM2002; Doosan Co. Ltd.) to a diameter of 0.2–0.4 mm. A controlled quality of distilled water (10.8 mL) was added slowly, while stirring the solution magnetically to allow the hydrolysis reaction to take place and form a gel. The gel was formed by the removal of the solvent and water from the solution under vacuum in a rotary evaporator (ES600; Wooil E.R.S. Co. Ltd.), which also aided a more uniform deposition of the TiO_2 nanoparticles onto the CNSP. The experiment was repeated with different amounts of CNSP (0, 60, 80, 100, and 120 g). The convention used for naming the new composites was pure TiO_2, TCNSP60, TCNSP80, TCNSP100, TCNSP120, and CNSP, according to the level of CNSP loading on titanium dioxide sol (i.e., TCNSP100 = Titanium-n-butoxide [34.04 mL] + diethanolamine [10.4 mL] + ethanol [259.28 mL] + CNSP 100 g + distilled water [10.8 mL]).

Granulation process (semiautomated mass production line)

A semiautomated mass production line (AMPL) was used as the granulation process in this study. This process produced a pelletized form of TCNSP composite powder from the sol-gel technique. In addition, this process has the capacity to produce a sufficient quantity of TCNSP composite pellets with sufficient strength for commercialization. The semi-AMPL process used for granulation of TCNSP composites consists of four operations—(1) kneading, (2) roller compaction, (3) pelletization, and (4) mechanofusion process.

Production of the TCNSP composite pellets

The semi-AMPL was adapted for producing the TCNSP composite pellets. Distilled water (10 wt%) was added into the prepared TCNSP composite along with wheat flour (10 wt%) that was found from preliminary trials to be a suitable material to act as a binder. The flour was found to aid the formation of the spherical pellets in the later stages of production. The material was kneaded using a kneading machine, which had four arms for uniformly kneading flour

Table 1. Composition Analysis Results of Coconut Shell Powder

Extractives, %		*Lignin, %*		*Carbohydrates, %*		*Ash, %*	
Cold water	2.87	Klason	39.70	Holocellulse	58.02		
Hot water	0.73	Acid soluble	2.06	Cellulose	44.95		
1% NaOH	20.40			Hemicellulose	13.07		
Alcohol-benzene	1.28						
Total	25.28					Total	8.28

with CNSP, for 1–5 min, until the required shape was developed. The TCNSP composite dough was then transferred to the rolling machine for de-aeration; 2–5 runs were required to achieve the desired de-aerated material. This was then fed into a rotating drum of the pellet former, where the TCNSP composite pellet spheres (diameter of 2–4 mm) were produced. The pellets were then transferred to a mechanofusion machine agitator for consolidation and to enhance the crush strength of composites. Figure 1 shows the overall flow diagram for the production of spherical TCNSP composite pellets.

Heat treatment of TCNSP composite pellets

The TCNSP composite pellets generated from the semi-AMPL were dried at 50°C for 5 h in an oven to avoid cracking of the pellet's surface. The dried pellets were calcinated at various temperatures ranging 500–800°C for 2 h at a heating rate of 10°C/min under N_2 gas flow (400 mL/min) in a furnace. The pellets were then left inside the furnace to cool down to around 150°C, and then removed and placed in a desiccator for cooling to room temperature. The pellets were then washed by deionized water and dried before use.

Characterization of TCNSP composite pellets

The morphology and pore structure of TCNSP composites were analyzed using a scanning electron microscope (SEM; S-570/Hitachi) with energy dispersive X-ray spectroscopy (EDS). The crystal composition and crystallite sizes of each sample were determined using X-ray diffraction (XRD) (Philips X'pert PRO MRD). Cu Kα irradiation (wavelength = 0.154 nm) at a scan rate of 0.005° to determine the crystalline phase; the crystallite size was calculated from the Scherrer equation. Diffraction patterns were taken over the 2θ range from 20° to 79.99°. The specific surface area of TCNSP was analyzed using a Quantachrome NOVA 2200e by the Brunauer-Emmett-Teller (BET) equation using the adsorption data. The crush strength of the individual granules was measured as the maximum load applied to break the granule using a desk-top-type Universal Testing Machine (Shimadzu-AGS-5KN).

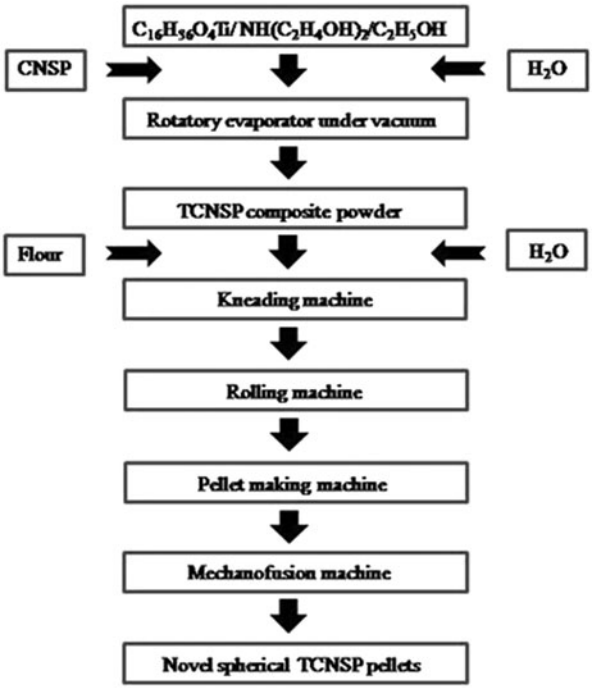

FIG. 1. Preparation steps for novel TiO_2–coconut shell powder (TCNSP) composite pellets using semiautomated mass production line.

CBZ drug sample preparation

CBZ powder was supplied by Sigma, and used without further purification. Fifty millligrams of CBZ was dissolved into 50 mg of high-performance liquid chromatography grade methanol (SK Chemical). The sample was stirred for 24 h to ensure a complete dissolution (Behera *et al.*, 2010). Dissolved samples were stored at 4°C and used within a month of preparation. The sample solutions for all adsorption and photocatalysis reaction tests were prepared by adding the stock solution to ultrapure water to achieve the desired concentration levels. The concentrations of the CBZ were determined using a UV-visible spectrophotometer (Shimadzu UV-1601) at 284 nm. All experiments were carried out in triplicate.

Adsorption and photocatalytic reaction experiments

The adsorption and the photocatalytic reaction of the target compound were conducted in a fixed bed adsorption–photocatalytic reactor coupled with a circulative flow mode (Fig. 2). The experimental apparatus consists of a reactor of square cross section of 11-cm and 27-cm height operating with a recirculation pump. A stainless steel gauze was placed in the reactor to stop elution of the TCNSP composite pellets. The UV light source used in this study was a TUV11W germicidal UVC lamp (Philips) providing a principal output at 254 nm UVC radiation. All parts of the reactor

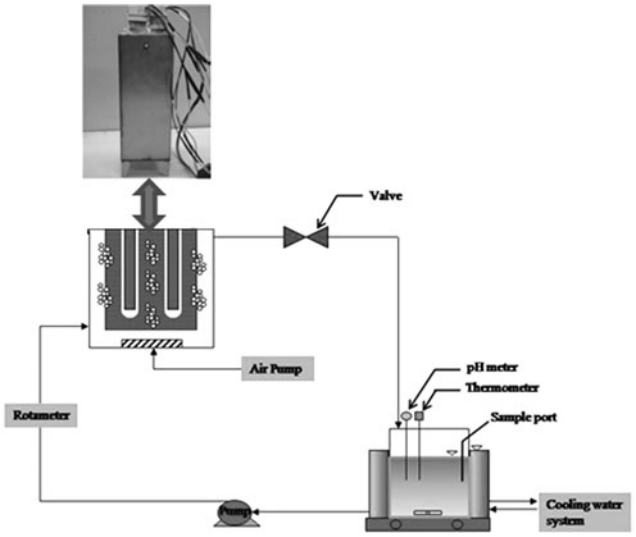

FIG. 2. Schematic diagram of the fixed bed photocatalytic reactor coupled with circulative flow mode.

were made from stainless steel to enhance the refracted light intensity and to repress organic compound attachment on the surface of the reactor. To induce satisfactory mixing of the solution, a magnetic stirrer was used in the reservoir tank of 4 L. The mixture was then irradiated under UVC intensity of 10.5 mW/cm^2 for 60 min. The total volume of the withdrawn samples was less than 2% (by volume) of the circulated solution. About 3.6 L of an aqueous solution was loaded in the reservoir of a photocatalytic reaction system and contacted with TCNSP composites in the concentration range of 60–120 g/L. A recirculation flow rate of 0.2 L/min led to a residence time in the absorbed and irradiated reactor of 10 s. A constant bottom-to-top oxygen flow was supplied using an air pump, which acted as an electron scavenger to prevent the recombination of electron-hole pairs. The temperature of the system was maintained constant at ~20°C by a cooling water bath surrounding the reservoir. The pH of the solution was adjusted from pH 3 to 11 by H_2SO_4 and NaOH, respectively.

Optimum condition of the TCNSP composite preparation

RSM and CCD models were used to investigate the optimum conditions for preparation of the TCNSP composites. The variables (independent factors) were the calcination temperature (x_1) and CNSP loading amount (x_2). The remaining concentration of the target compound was considered as the response (dependent factors). The experimental ranges and the levels of the independent variables for TCNSP composites are shown in Table 2.

A two factor and two-level factorial with a full fraction design was used. Thus, the total number of experimental runs calculated was 14 runs. Data were analyzed to fit the following polynomial equation to Y (remaining concentration of the target compound) where b_0 is constant, b_i is the linear coefficient, b_{ii} is the quadratic coefficient, b_{ij} is the interaction, and x_i and x_j are the independent variables.

$$Y = b_0 + \sum b_i x_i + \sum b_{ii} x_i^2 \sum b_{ij} x_i x_j \quad (1)$$

Minitab® software 16 (Minitab, Inc.) was used for analysis of variance (ANOVA) and regression coefficient calculations. The predicted model was then compared with the experimental results.

Results and Discussion

Crush strength of TCNSP composites

For applications dealing with water purification, the mechanical stability and durability of the TCNSP composites are very important aspects. The effect of the production variables was investigated to determine the optimum preparation conditions required. Figure 3a shows the effect of kneading time on the crush strength of the TCNSP composite. The mean initial crush strength of the TCNSP composite granule was 0.42 N. As the kneading time increased, the crush strength of the TCNSP composite increased accordingly. However, there was a slight decrease in the crush strength after 3 min, therefore, this was considered to be the optimum time required to achieve the maximum required strength. Moreover, the TCNSP dough, generated from the kneading process, was put through the rolling process that improved the crush strength of pellets.

The kneading process removes most of the trapped air within TCNSP composites. It is essential that the remaining air in the composite is removed as it generates cracks on pellet surfaces on the later stages of composite production. The surface cracks not only impact upon the production efficiency of the composite, but also its crush strength,

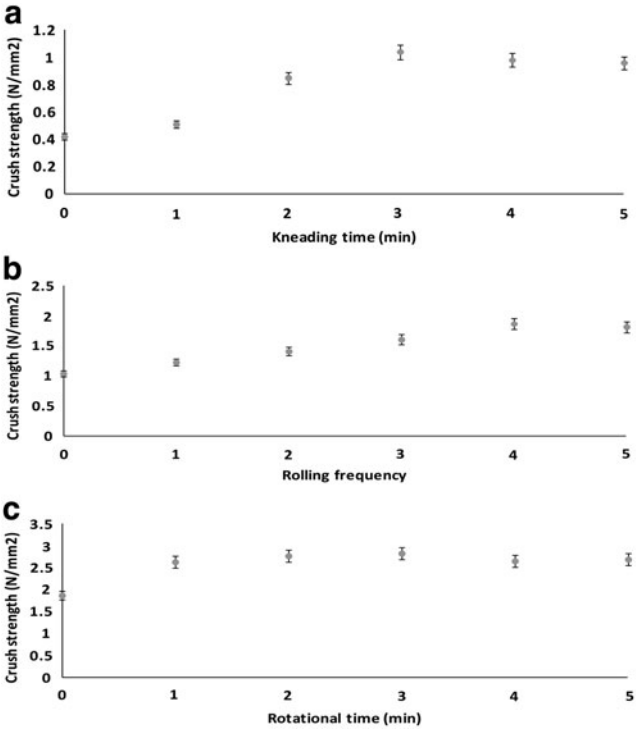

FIG. 3. Effect of various factors on crush strength of spherical TCNSP100 composites: **(a)** kneading time, **(b)** rolling frequency, and **(c)** rotational time.

Table 2. Experimental Ranges and Levels of Independent Variables

		Ranges and levels				
Symbol	*Variables*	*−2*	*−1*	*0*	*1*	*2*
x_1	Calcination temperature (°C)	500	600	700	800	900
x_2	CNSP amount (g)	60	80	100	120	Only CNSP

CNSP, coconut shell powder.

which significantly affects the water treatment performance of the composite. The rolling process does not simply compresses particles together to reduce the physical size of composites, but it also removes moisture and any trapped air.

Figure 3b shows the effect of the rolling frequency on the crush strength of the TCNSP composite. The initial crush strength of the spherical TCNSP composite was 1.04 N/granule, which was determined from 3 min of kneading time. Increasing the rolling frequency improved the crush strength of the material. The optimal conditions were reached after 4 runs in the rolling machine (each kneading process takes ~1 min).

The initial crush strength of spherical TCNSP composites was 1.87 N/granule, which was determined by the rolling frequency experiment. The composite crush strength was improved by bombarding pellets against each other via mechanofusion. The crush strength of the spherical TCNSP composite increased within 3 min; there was a slight decrease with longer consolidation times (Fig. 3c).

Calcination temperature of TCNSP composites

To prepare the TCNSP composites to have a photocatalytic function and adsorption ability, a calcination process was utilized using time heat treatment under various temperatures ranging from 500°C to 800°C. The purpose of the calcination process for the CNSP was to create an initial porosity in the char as well as to transfer the TiO_2 crystallite phase from amorphous to anatase. Previous studies have shown that high calcination temperatures may result in a greater amount of volatiles being released from the raw material, which eventually influences the porosity of the product (Daun *et al.*, 2000; Xiang *et al.*, 2012). In addition, the amorphous phase of TiO_2 crystallizes into the anatase phase, and then transforms into the rutile phase as the calcination temperature increased. Li *et al.* (2007) reported that both the anatase and rutile phase were evident for the TiO_2/activated carbon (AC) composite when it was heated to 500°C and was completely transferred to the rutile phase at 700°C.

Figure 4 shows the SEM images of the TCNSP100 composite at different calcination temperatures. It can be seen from Fig. 4 confirmed by XRD results (Fig. 5) that nanotitanium dioxide particles were homogeneously dispersed within the CNSP. To determine if the titanium dioxide was successfully distributed within the coconut shell char, EDS analysis was employed in conjunction with SEM. A typical EDS pattern is shown in Fig. 6 and the elemental composition of the TCNSP composite was shown to be 60.92% C, 26.82% O, and 12.26% Ti, confirming the presence of titanium dioxide on the surface of the char.

Images in Fig. 4 illustrate the spherical nature of the particles, with large particles formed from aggregates of finer material. The specific surface area of TCNSP100 increased with increasing calcination temperature. It was also observed that discernible pores were present at the surface of TCNSP100 composites.

Table 3 illustrates that the BET surface of the TCNSP100 composite increased from 316 m^2/g at 500°C to 454 m^2/g at 700°C and also that the pore volume, porosity, and crush strength of spherical TCNSP100 composites increased with increasing calcination temperature from 500°C to 700°C. According to the pyrolysis results, the hemicellulose, cellulose, and lignin within the coconut shells may cause a polymerization reaction during the calcination process (Li *et al.*, 2008). The BET surface area of TCNSP100 increased with increasing calcination temperature and decreased for temperatures over 800°C. This can be attributed to the fact that an

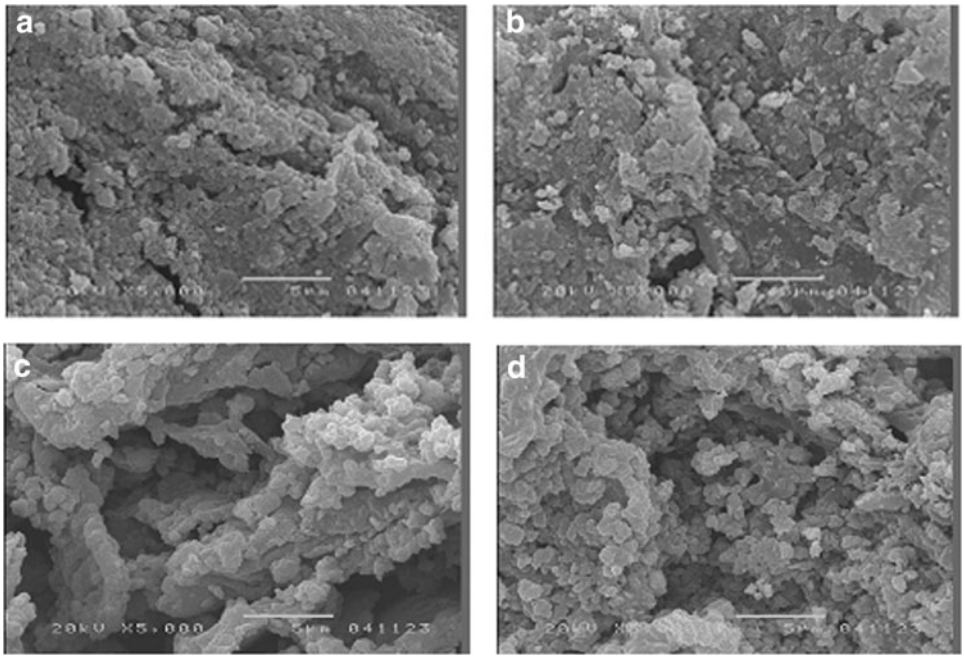

FIG. 4. Scanning electron microscope (SEM) images of the spherical TCNSP100 composites at different calcinated temperatures: **(a)** 500°C, **(b)** 600°C, **(c)** 700°C, and **(d)** 800°C.

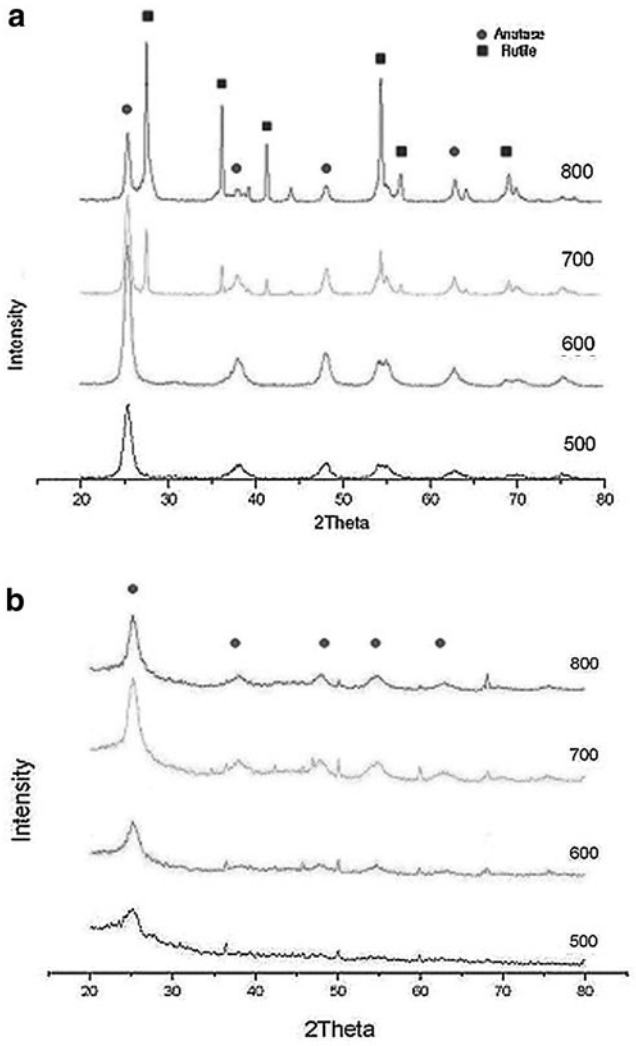

FIG. 5. X-ray diffraction patterns of **(a)** pure titanium dioxide and **(b)** TCNSP100 at different calcinated temperatures.

increase in calcination temperature would result in increased polymerization reactions within the spherical TCNSP100 composite. However, the BET surface area decreased for temperatures above 700°C, which may be caused by the shrinkage of TiO_2 nanoparticles or rapid growth of TiO_2 crystallites on the spherical TCNSP composites. These data are consistent with (Kim *et al.*, 2007) who reported that when the calcination temperature increased, the BET surface area of the TiO_2/di-block copolymer composites decreased due to the crystallization of TiO_2, subsequent crystal growth, and the collapse of the porous structure.

Porosity of the TCNSP composites (Table 3) showed a similar trend with the pore volume of the composites. With increasing calcination temperature, the porosity of the TCNSP100 slightly increased, however, this decreased after 800°C. Table 3 shows the crush strength of the TCNSP100 with different calcination temperatures. The crush strength of the spherical TCNSP composite decreased slightly with increasing calcination temperature. Jing *et al.* (2009) showed that increasing calcination temperature results in a greater amount of volatiles to be released from the raw material, which may eventually influence the product yield and porosity. Therefore, greater porosity causes less crush strength of TCNSP. However, in the case of the 800°C calcination temperature, the crush strength also decreased even though the porosity decreased. This was probably caused by the collapse of the porous structure caused by high calcination temperature.

XRD patterns of spherical TCNSP100 composites with different calcination temperatures are shown in Fig. 5. With increasing calcination temperature from 500°C to 800°C, the anatase peak of TCNSP100 composites became narrower and higher. It can be speculated that the TiO_2 crystals trend to a more perfect anatase type, and then grow into larger particles. The anatase crystallite size of the TCNSP100 composite increased rapidly from 2.37 to 15.11 nm with increasing calcination temperature from 500°C to 800°C. With increased calcination temperatures, the stress and strain are eliminated with improved crystallinity as indicated from the XRD data. This result is in agreement with Li *et al.* (2005) and Lu *et al.* (2012), who found that the increase of crystallite sizes with increasing calcination temperature was a significant factor for growth of the crystallites. All TCNSP samples calcinated at temperatures up to 800°C retained the structure of anatase and there was no rutile peak (as shown in Fig. 6). Therefore, it is possible that the phase structure of spherical TCNSP composites was stable with CNSP loading (i.e., no or little transformation from anatase to rutile phase took place). This may be attributed to the substrate (CNSP) acting as a barrier for phase transformation.

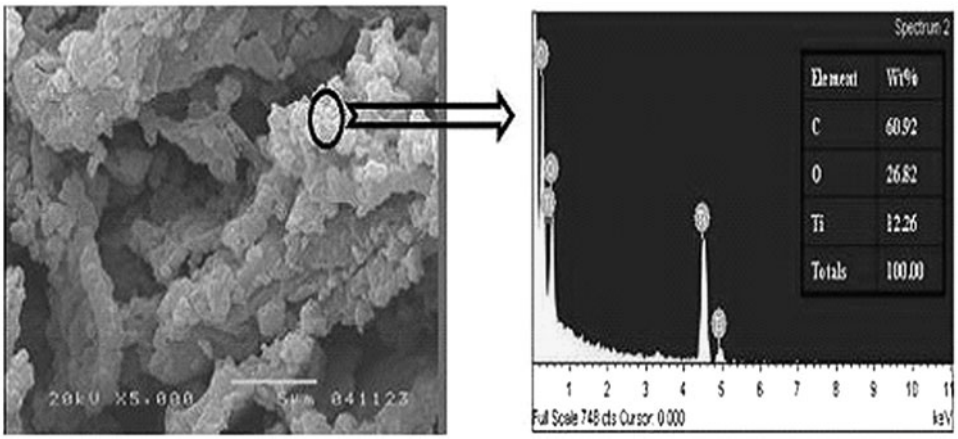

FIG. 6. Energy dispersive X-ray spectroscopy (EDS) spectrum of TCNSP100 composites calcinated at 700°C.

Table 3. Characteristics and Crush Strength of Spherical TiO_2–Coconut Shell Powder 100 Composites with Different Calcination Temperatures

Calcination temperature (°C)	*BET (m^2/g)*	*Crush strength (N/granule)*	*Pore volume (cm^3/g)*	*Pore size (nm)*	*Porosity (%)*	*Anatase crystallite size (nm)*
500	316	26.3 ± 2.8	0.15	3.1	65.56	2.37
600	431	26.1 ± 3.1	0.18	2.8	66.56	4.12
700	454	25.7 ± 3.4	0.24	2.2	66.87	8.39
800	405	20.6 ± 2.2	0.19	2.4	64.13	15.11

BET, Brunauer-Emmett-Teller.

Effect of CNSP loading amount

Another parameter that will influence the final characteristics of the TCNSP material is the TiO_2:CNSP ratio. Li *et al.* (2005) demonstrated that increasing the amount of TiO_2 loading in TiO_2/AC composites would decrease the BET surface area of composites. It is clear that the average specific surface area of the TiO_2/AC strongly depends on the ratio of TiO_2 and AC. Figure 7 illustrates the SEM images of the surface of the pure TiO_2 and TCNSP composite with different CNSP loading prepared at a 700°C calcination temperature. The surface of pure TiO_2 is relatively smooth and the particles

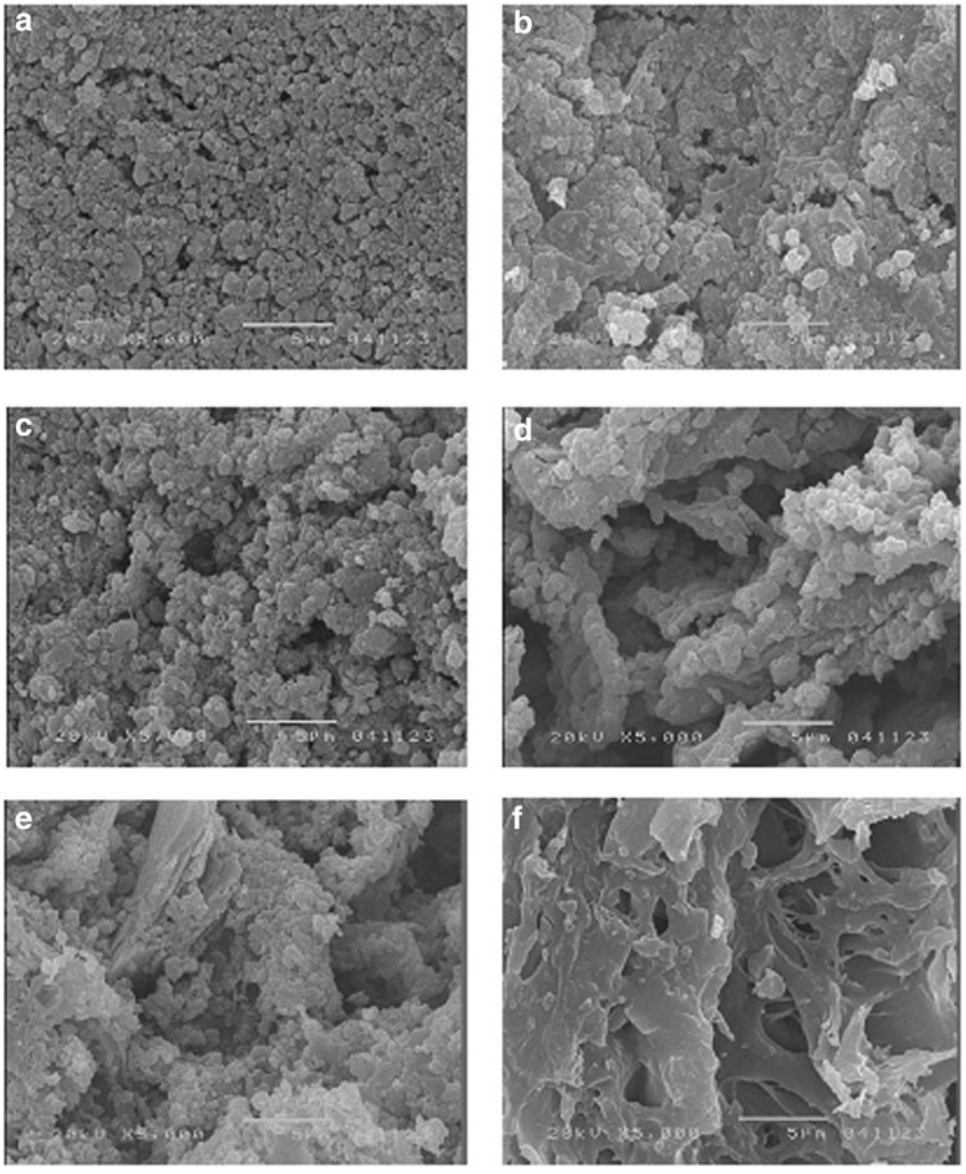

FIG. 7. SEM images of pure titanium dioxide and spherical TCNSP composites with different amounts of loading coconut shell powder (CNSP) prepared at 700°C calcination temperature: **(a)** pure titanium dioxide, **(b)** TCNSP60, **(c)** TCNSP80, **(d)** TCNSP100, **(e)** TCNSP120, and **(f)** CNSP.

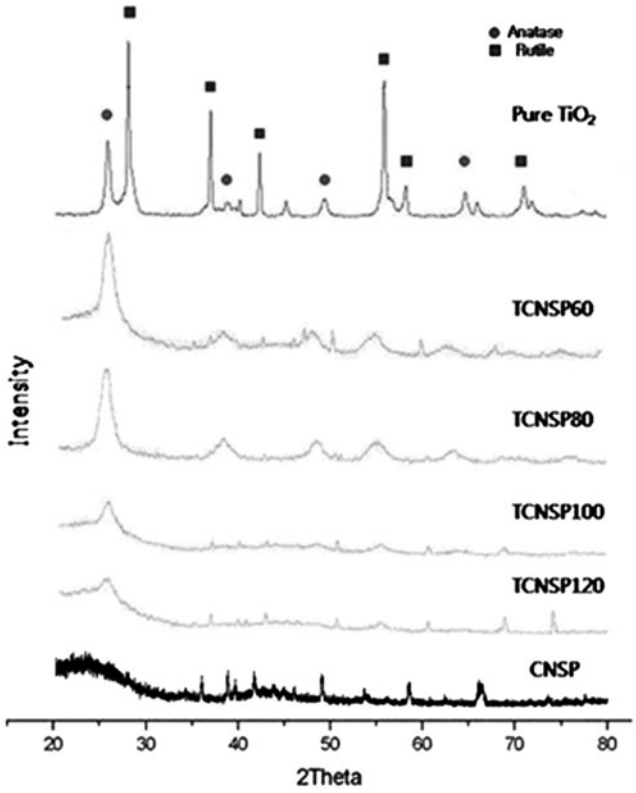

FIG. 8. XRD patterns of spherical TCNSP composites with different CNSP loading amounts and pure TiO_2 particles at 700°C calcination temperature.

are aggregated densely compared to the other samples. With increasing CNSP loading, the small particles agglomerated together leading to the formation of a porous surface on the composites. It can be observed that discernible pores were present at the surface of TCNSP60, 80, 100, and 120 (Fig. 7). As shown in Fig. 7, the TiO_2 particles were well-dispersed on the CNSP surface. This can be attributed to the method of deposition TiO_2 particles onto CNSP under the rotatory vacuum evaporator aiding a more uniform and firm deposition of TiO_2 particles onto the CNSP. As the nonuniformity of large-sized aggregation of the coating particles is avoided, the residual air, water, or solvents on the CNSP can be removed more thoroughly (Ao *et al.*, 2008). The XRD patterns of spherical TCNSP composites, with different CNSP loading amounts (TCNSP60, 80, 100, and 120) as well as pure TiO_2 particles, at 700°C calcination temperature are shown in Fig. 8. In comparison with pure TiO_2 XRD results, the crystallites of all TCNSP composites formed the anatase phase at 700°C calcination temperature (Fig. 8). As the amount of CNSP loading increased from TCNSP60 to TCNSP120 under the same calcination temperature, the peak at 25.3° became wider and shorter, implying that TiO_2 crystals trend to the amorphous phase and grew into smaller particles. This phenomenon may have been caused by the increasing amount of CNSP loading, which restricts the transformation of TiO_2 from anatase to the rutile phase due to the hindrance of interfacial energy between TiO_2 and CNSP.

Table 4 shows the BET surface area, pore size, pore volume, and crush strength of pure TiO_2 and spherical TCNSP composites prepared at a 700°C calcination temperature for different CNSP loading. The BET surface areas of the TCNSP composites were higher compared with CNSP char, although this was higher than pure TiO_2. As indicated in Fig. 7, the particles on the surface of pure TiO_2 were densely aggregated compared with TCNSP composites. This result is in agreement with results reported by Li *et al.* (2005), who investigated the TiO_2-coated activated carbon composites and found a higher BET surface area compared with pure TiO_2 and pure activated carbon. Table 4 also shows the porosity and crush strength of the TCNSP composite, pure TiO_2, and pure CNSP char. With increasing CNSP loading amount, the porosity and crush strength of the TCNSP composites increased.

Drug removal

Effect of calcination temperature. To evaluate the adsorption and photocatalytic reaction of TCNSP composites calcinated at 700°C with different CNSP loading, bench-scale experiments were undertaken in a fixed bed reactor coupled with a circulative flow mode (Fig. 2) under UVC irradiation for the removal of CBZ. Figure 9 shows the effect of calcination temperature of TCNSP100 composites on the photocatalytic degradation rate. It is evident in Fig. 9 that all TCNSP composites had a higher adsorption and photocatalytic activity than pure TiO_2 and CNSP char. The TCNSP100 calcinated at 700°C had a larger surface area (454 m^2/g) than the other materials, indicating that it may have a better adsorption activity. Regarding the effect of pore size, materials having a smaller pore size showed a higher adsorption and

Table 4. Characteristics and Crush Strength of Pure TiO_2 and TiO_2–Coconut Shell Powder Composite with Different Coconut Shell Powder Loading Amounts

Composite	*BET (m^2/g)*	*Crush strength (N/granule)*	*Pore volume (cm^3/g)*	*Pore size (nm)*	*Porosity (%)*	*Anatase crystallite size (nm)*
Pure TiO_2	83	8.10 ± 2.4	—	—	52.88	15.23
TCNSP60	372	12.6 ± 2.0	0.19	2.4	64.67	14.68
TCNSP80	404	24.7 ± 3.1	0.20	2.2	67.82	10.08
TCNSP100	454	25.7 ± 3.4	0.24	2.2	68.94	6.98
TCNSP120	412	33.1 ± 2.5	0.23	2.1	68.45	3.65
CNSP	289	38.8 ± 2.5	0.19	2.7	63.21	—

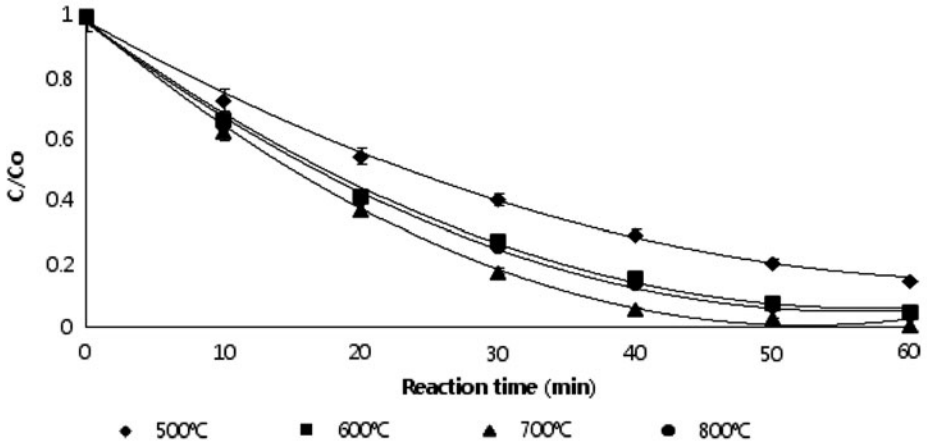

FIG. 9. Effect of calcination temperature on adsorption and photocatalytic degradation rates for TCNSP100 composites (initial concentration of carbamazepine [CBZ] = 10 mg/L, TCNSP100 composite concentration = 120 g/L, pH = 7, irradiation time = 60 min, oxygen concentration = 24 mg/L, UVC intensity = 10.5 mW/cm^2, temperature = 20°C).

photocatalytic activity (Table 5 and Fig. 10). Thus, TiO_2 with small pore sizes degrade adsorbed substances more readily and effectively. Furthermore, higher calcination temperatures favored the formation of more stable TiO_2 crystallites of the anatase phase and a larger crystallite size. It has been commonly accepted that a smaller crystallite size corresponds to a higher redox ability as a smaller crystallite size induces a larger band gap (Pecchi *et al.*, 2001; Kim *et al.*, 2007). However, the performance of TCNSP100 calcinated at 800°C was better compared with TCNSP100 calcinated at 600°C, although the latter had a smaller crystallite size, suggesting that the crystallite structure was more important than the crystallite size. However, TCNSP100 calcinated at 700°C, which had a smaller size, performed better than TCNSP100 calcinated at 800°C, which implies that the calcination temperature of 700°C was the optimum temperature. The results demonstrate that the surface area, pore-size distribution, and crystallite structure and size of the TCNSP100 composites had significant influence on the adsorption and photocatalytic activity performance.

Table 5. Predicted Remaining Concentration of Carbamazepine Obtained by Central Composite Design

Run order	*Pt type*	*Blocks*	*Temp. (°C) x_1*	*CNSP (g) x_2*	*Experimental RC (mg/L)*	*Predicted RC (mg/L)*
1	0	1	700	100	1.8	1.88
2	1	1	600	80	3.5	2.74
3	1	1	800	80	3.1	2.54
4	0	1	700	100	1.8	1.88
5	0	1	700	100	1.8	1.88
6	1	1	800	120	2.7	3.00
7	1	1	600	120	3.8	3.90
8	0	2	700	100	1.8	1.88
9	−1	2	500	100	4.1	4.31
10	−1	2	900	100	3.2	3.21
11	0	2	700	100	1.8	1.88
12	−1	2	700	60	3.3	3.85
13	0	2	700	100	1.8	1.88
14	−1	2	700	Only CNSP	5.8	5.48

RC, remaining concentration (mg/L).

CCD experiments. Table 5 shows the CCD with calcination temperature and CNSP loading amount for 14 experimental runs. It can be observed that the predicted results were close to the experimental results indicating the applicability of the proposed design. The experimental relationship between the responses and independent variables were attained and expressed using the following second-order polynomial equations, where x_1 and x_2 represent the calcination temperature and CNSP loading amount, respectively. ANOVA results of this model for CBZ removal are summarized in Table 6.

$$Y = 36.19 - 0.0601x_1 - 0.2669x_2 + 0.0017x_2x_2 - 0.0001x_1x_2 \quad (2)$$

Table 5 illustrates that the regression model was highly significant, as is evident from the calculated Fisher's *F*-value (18.45) and a very low probability value ($p = 0.000$). It has been reported that a higher value of *F* indicates that most of the variation in the response can be explained by the regression equation and the associated *p* value is used to estimate whether *F* is large enough to indicate statistical significance (Azargohar and Dalai, 2005). If the value of *F* is high and the value of *p* is less than 0.05, it means the model is statistically significant (Talat, 2009). The coefficient of determination, the R^2 value was 92.02% for the remaining concentration, indicating that the correlation is good for predicting the performance of the system. After performing statistical analyses, the response surface analysis was carried out to find the optimum conditions for the remaining concentrations of CBZ. Figure 11 shows the response surface plot and contour for a 30-min reaction time for the optimization conditions to prepare a TCNSP composite for CBZ removal. The remaining concentration of CBZ decreased when the calcination temperature increased from 500°C to 700°C and the CNSP loading amount increased from 60 to 100 g.

Response optimization helps to identify the factor settings that optimize a single response or a set of responses (Hasan *et al.*, 2009). Figure 12 shows the optimization curve of the TCNSP preparation process. The remaining concentration of

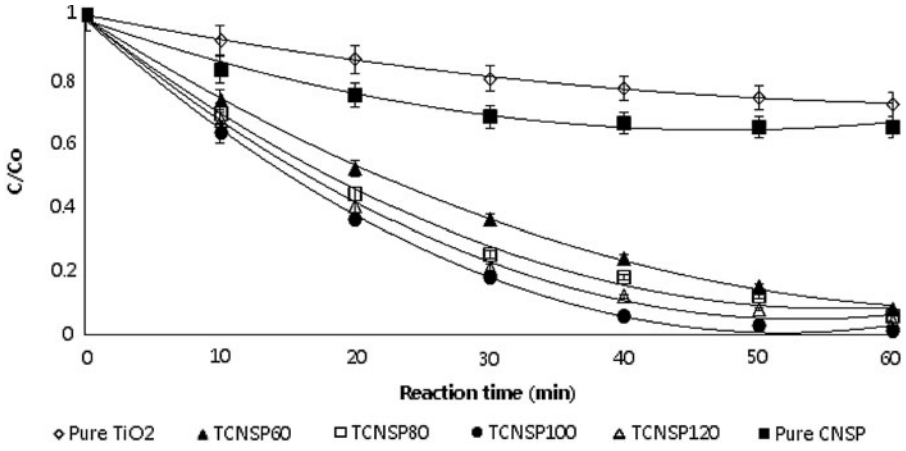

FIG. 10. Effect of CNSP loading amount on adsorption and photocatalytic degradation rates (initial concentration of CBZ = 10 mg/L, TCNSP100 composite concentration = 120 g/L, pH = 7, irradiation time = 60 min, oxygen concentration = 24 mg/L, UVC intensity = 10.5 mW/cm^2, temperature = 20°C).

Table 6. Analysis of Variance for Remaining Concentration Versus Calcination Temperature and Coconut Shell Powder Loading Amount

Source of variations	*Sum of squares*	*Degree of freedom*	*Adjusted mean square*	F-*value*	p-*Value*
Regression	17.12	5	3.424	18.5	0.000
Linear	2.632	2	1.316	7.09	0.017
Square	14.09	2	7.044	38.0	0.000
Interaction	0.123	1	0.123	0.66	0.440
Residual error	1.485	8	0.186		
Total	18.60	13			

$R^2 = 92.02\%$, Adjusted $R^2 = 87.03\%$, $p < 0.05$ significant.

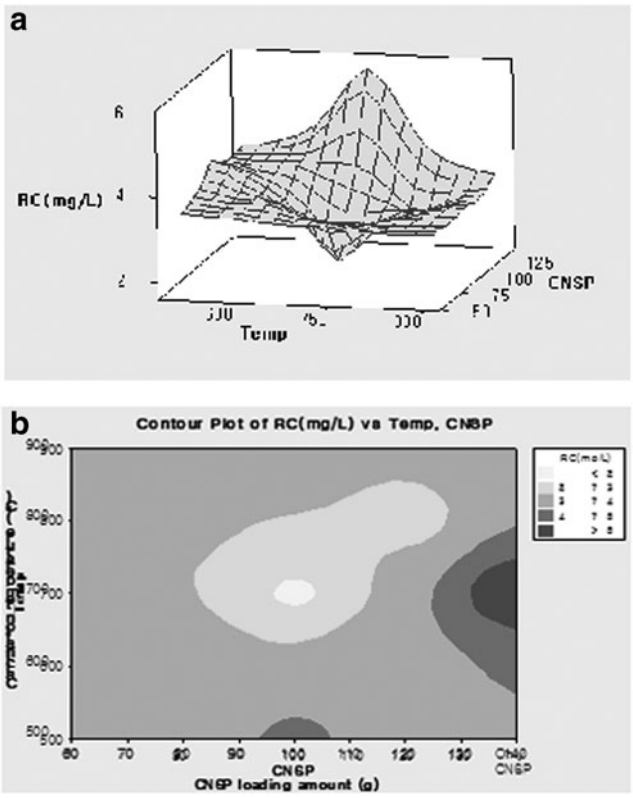

FIG. 11. Response surface **(a)** and contour plot **(b)** of remaining concentrations of carbamazepine at $t = 30$ min as a function of calcination temperature and CNSP loading amount.

CBZ was defined as the minimum value to achieve the optimum preparation conditions of the TCNSP composite. These results were obtained from the Response Optimizer tool in Minitab software 16. The optimum condition, that is, the best combination of factor settings for achieving the optimum response, was found to be a calcination temperature of 726°C and CNSP loading amount of 94.75 g for a predicted response of 1.79 mg/L of the remaining concentration for a 30-min reaction time with a desirability score of 0.96.

As compared with the results obtained from one-factor-at-a-time experiments (Figs. 5 and 8), the values were approximated to the nearest condition of these values and the following experimental parameters were set as the optimum: 700°C calcination temperature and 100 g of CNSP loading amount. These results indicate that the quadratic regression model [Equation (2)] reasonably optimized the variable conditions and predicted the preparation of TCNPS composites.

Conclusion

Novel TCNSP composites consisting of TiO_2/CNSP were successfully prepared using the controlled sol-gel method with a subsequent heat treatment. Calcinated TCNSP composites had higher removal efficiency (98%) than pure TiO_2 (23%) and CNSP (34%) within a 40-min

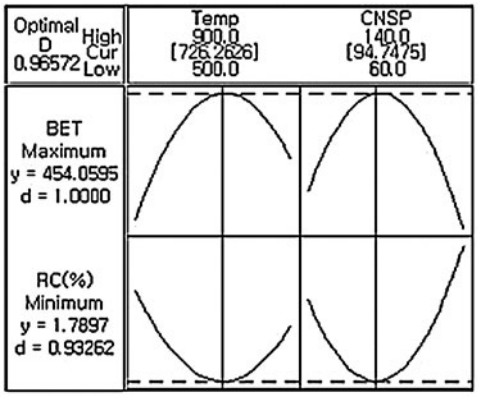

FIG. 12. Optimization curve for the preparation conditions of TCNSP composites.

reaction time. The optimum values for the preparation of TCNSP composites, obtained by the RSM and CCD model, were found to be 726°C calcination temperature, 94.8 g CNSP loading amount for a predicted response of 1.79 mg/L of remaining concentration after a 30-min reaction time. In comparison, for data obtained by the one-factor-at-a-time experiments, RSM based on CCD could be effectively adopted to optimize the preparation of TCNSP composites. Furthermore, the optimization using a RSM and CCD can save the time and effort by the estimation on the optimum conditions of TCNSP composite preparation.

Acknowledgments

The Wooil E.R.S. Company of Korea financially supported this project (New technology Project-WI20090216). The authors are also grateful to the Kangwon National University in Korea for support of production equipment. Authors are also grateful for the Qatar University Internal Grant Fund QUUG-CENG-CH-09/10-4.

Author Disclosure Statement

No competing financial interests exist.

References

Acharya, J., Sahu, J.N., Sahoo, B.K., Mohanty, C.R., and Meikap, B.C. (2009). Removal of chromium (VI) from wastewater by activated carbon developed from tamarind wood activated with zinc chloride. *Chem. Eng. J.* 150, 25.

Ao, Y., Xu, J., Shen, X., and Yuan, C. (2008). Low temperature preparation of anatage TiO_2-coated activated carbon. *Colloid Surf. A* 312, 125.

Azargohar, R., and Dalai, A.K. (2005). Production of activated carbon from Luscar char: Experimental and modeling studies. *Micropor. Mesopor. Mater.* 85, 219.

Behera, S.K., Oh, S.Y., and Park, H.S. (2010). Sorption of triclosan onto activated carbon, kaolinite and montmorillonite: Effects of pH, ionic strength, and humic acid. *J. Hazard. Mater.* 179, 684.

Bouna, L., Rhouta, B., Amjoud, M., Maury, F., Lafont, M.C., Jada, A., Senocq, F., and Daoudi, L. (2011). Synthesis, characterization and photocatalytic activity of TiO_2 supported natural palygorskite microfibers. *Appl. Clay Sci.* 52, 301.

Calisto, V., and Esteves, V.I. (2012). Adsorption of the antiepileptic carbamazepine onto agricultural soils. *J. Environ. Monit.* 14, 1597.

Chen, Y., and Dionysiou, D.D. (2006). TiO_2 photocatalytic films on stainless steel: The role of Degussa P-25 in modified sol-gel methods. *Appl. Catal. B* 62, 255.

Daun, W.M.A., Ali, W.S.W., and Sulaiman, M.Z. (2000). The effects of carbonization temperature on pore development in palm-shell-based activated carbon. *Carbon* 38, 1925.

Hasan, S.H., Srivastava, P., and Talat, M. (2009). Biosorption of Pb(II) from water using biomass of *Aeromonas hydrophila*: Central composite design for optimization of process variables. *J. Hazard. Mater.* 168, 1155.

Iwasaki, M., Hara, M., Kawada, H., Tada, H., and Ito, S. (2010). Cobalt ion-doped TiO_2 photocatalyst response to visible light. *J. Colloid Interface Sci.* 224, 202.

Jing, M.X., Jiang, X.Q., Li, W.X., Li, D.H., and Wang, Z. (2009). Preparation and photocatalytic activity of mesoporous TiO_2 microspheres. *Micro. Nanosyst.* 1, 12.

Kim, S.D., Cho, J., Kim, I.S., Vanderford, B.J., and Synder, S.A. (2007). Occurrence and removal of pharmaceuticals and endocrine disruptors in South Korean surface, drinking, and waste waters. *Water Res.* 41, 1013.

Le, H., Linh, L., Chin, S., and Jurng, J. (2012). Photocatalytic degradation of methylene blue by a combination of TiO_2-anatase and coconut shell activated carbon. *Powder Technol.* 225, 167.

Li, W., Yang, K., Peng, J., Zhang, L., Guo, S., and Xia, H. (2008). Effects of carbonization temperatures on characteristics of porosity in coconut shell chars and activated carbons derived from carbonized coconut shell chars. *Indust. Crops Prod.* 28, 190.

Li, Y., Li, X., Li, J., and Yin, J. (2005). TiO_2-coated active carbon composites with increased photocatalytic activity prepared by a properly controlled sol-gel method. *Mater. Lett.* 59, 2659.

Li, Y., Zhang, S., Yu, Q., and Yin, W. (2007). The effects of activated carbon supports on the structure and properties of TiO_2 nanoparticles prepared by a sol-gel method. *Appl. Surf. Sci.* 253, 9254.

Liu, J., Dong, M., Zuo, S., and Yu, Y. (2009). Solvothermal preparation of TiO_2/montmorillonite and photocatalytic activity. *Appl. Clay Sci.* 43, 156.

Lu, S., Wang, Q., Buekens, A.G., Yan, J., Li, X., and Cen, K. (2012). Photocatalytic decomposition of gaseous 1,2-dichlorobenzene on TiO_2 films: Effect of ozone addition. *Chem. Eng. J.* 195–196, 233.

Nieto-Suárez, M., Palmisano, G., Ferrer, M.L., Gutiérrez, M., Yurdakal, S., Augugliaro, V., Pagliaro, M., and del Monte, F. (2009). Self-assembled titania-silica-sepiolite based nanocomposites for water decontamination. *J. Mater. Chem.* 19, 2070.

Pecchi, G., Reyes, P., Sanhueza, P., and Villasenor, J. (2001). Photocatalytic degradation of pentachlorophenol on TiO_2 sol-gel catalysts. *Chemosphere* 43, 141.

Raj, K.J.A., and Vismanathan, B. (2009). Effect of surface area, pore volume and particle size of P25 titania on the phase transformation of anatase to rutile. *Indian J. Chem.* 48A, 1378.

Shankar, K., Tep, K.C., Mor, G.K., and Grimes, C.A. (2006). N-doped and N, F-codoped TiO_2 photoelectrodes: An electrochemical strategy to incorporate anionic dopants. *J. Phys. D: Appl. Phys.* 39, 2361.

Su, W., Zhou, L., and Zhou, Y.P. (2003). Preparation of microporous activated carbon from coconut shells without activating agents. *Carbon* 41, 861.

Talat, M. (2009). Detection of copper (II) in aqueous solution by immobilized urease obtained from agro-waste: Optimization of process variables. *Biotechnol. Biopro. Eng.* 14, 474.

Tamai, H., Katsu, N., Ono, K., and Yasuda, H. (2002). Simple preparation of TiO_2 particles dispersed activated carbons and their photo-sterilization activity. *J. Mater. Sci.* 37, 3175.

Valencia, S., Catano, F., Rios, L., Restrepo, G., and Marín, J. (2011). A new kinetic model for heterogeneous photocatalysis with titanium dioxide: Case of non-specific adsorption considering back reaction. *Appl. Catal. B* 104, 300.

Vogna, D., Marotta, R., Andreozzi, R., Napolitano, A., and d'Ischia, M. (2004). Kinetic and chemical assessment of the

UV/H_2O_2 treatment of antiepileptic drug carbamazepine. *Chemosphere* 54, 497.

Walker, G.M., and Weatherley, L.R. (1997). A simplified predictive model for biologically activated carbon fixed beds. *Process Biochem.* 32, 327.

Xiang, Q., Yu, J., and Jaroniec, M. (2012). Graphene-based semiconductor photocatalysts. *Chem. Soc. Rev.* 41, 782.

Yoneyama, H., and Torimoto, T. (2010). Titanium dioxide/adsorbent hybrid photocatalysts for photodestruction of organic substances of dilute concentrations. *Catal. Today* 58, 133.

Yu, Y., Wang, J., and Parr, J.F. (2012). Preparation and properties of TiO_2/fumed silica composite photocatalytic materials. *Procedia Eng.* 27, 448.

Zhang, Y., Geißen, S., and Gal, C. (2008). Carbamazepine and diclofenac: removal in wastewater treatment plants and occurrence in water bodies. *Chemosphere* 73, 1151.